JOURNAL OF AGRICULTURAL AND FOOD CHEMISTRY

Identification of Phenolic Compounds in Tissues of the Novel Olive Cultivar Hardy's Mammoth

DANIELLE RYAN,† MICHAEL ANTOLOVICH,† TONY HERLT,‡ PAUL D. PRENZLER,† SHIMON LAVEE,§ AND KEVIN ROBARDS*,†

School of Science and Technology and Farrer Centre, Charles Sturt University, Locked Bag 588, Wagga Wagga 2678, Australia, Research School of Chemistry, Australian National University, Canberra, ACT 0200, Australia, and Volcani Center 50-250, Bet Dagan and Hebrew University, Rehovot, Israel

A methodological approach to phenolic profiling making extensive use of LC-MS with extracted ion chromatograms was applied to extracts of five different olive tissues: pulp, seed, stone, new-season leaves, and old-season leaves. Tissue extracts of the cultivars Hardy's Mammoth, Corregiola, Verdale, and Manzanillo were analyzed by HPLC with UV and ESI MS detection. Chromatograms of samples of green Hardy's Mammoth drupes, a uniquely Australian olive cultivar, were dominated by a large, broad peak. This peak was not attributable to oleuropein, which is usually the dominant phenolic compound in green olive fruit, but the phenolic compound **I**. This compound was isolated by semipreparative HPLC and characterized by 1D- and 2D-NMR. Extraction studies showed that the compound was not likely to be an artifact of an enzymatic degradation process. Tritium labeling studies were used to establish a possible relationship between the biosynthesis of **I** and oleuropein.

KEYWORDS: Olive; phenol; tissues; identification; cultivar

INTRODUCTION

The complexity of the phenolic composition of *Olea europaea* has mandated analysis by high-performance techniques. Using high-performance liquid chromatography (HPLC), phenolic profiles of olives have been examined extensively (*1*−*10*) and, yet, there remain many unidentified compounds in a typical chromatogram. The most characteristic phenols in olive fruit are those esterified to the oleosides (*11*), and oleuropein is routinely identified as the major phenol (*5*, *12*, *13*).

Despite the importance of phenolic compounds to the quality of olive oil and their potential role in the physiological processes of olive trees (*5*−*7*), few studies have focused on the origin and fate of phenols within the olive plant. It has been established that different tissues contain distinctive phenolic compounds. For example, salidroside and nüzhenide have been isolated only from olive seeds (*14*, *15*). However, there have been few studies (*15*, *16*) in which the phenols in more than one tissue were characterized for a single variety of olive at a given time, although a recent review (*11*) presented a summary of data for various tissues. These data were a compilation of many discrete investigations involving different olive cultivars at different stages of maturity, and thus links between phenols in various tissues cannot be established.

To establish metabolic relationships between various phenolic compounds and tissues, a number of approaches may be adopted. The most direct is to use isotopically labeled compounds (e.g., enriched in ^{14}C); however, the difficulties of this approach with the Oleaceae family, including *Olea europaea*, have been documented (*17*). Another method involves comprehensive sampling of tissues during a fruiting season and monitoring phenolic profiles as a function of time. Utilizing this approach, we have discovered that oleuropein is not the major phenolic compound in green olive fruit of a number of cultivars grown in Australia, in direct contrast to the established literature (*5*−*7*, *13*). Given the significance of this finding, we report here the development of a methodological approach to phenolic profiling making extensive use of liquid chromatography−mass spectrometry (LC-MS) with extracted ion chromatograms from extracts of five different olive tissues: pulp, seed, stone, new-season leaves, and old-season leaves. Furthermore, the origins of the major phenolic compound in extracts from green fruit have been investigated using enzyme inhibition studies and ^{3}H labeling experiments.

MATERIALS AND METHODS

Chemical Reagents. Reagents from the following sources were used without further purification: acetic acid, acetonitrile, hydrochloric acid (32%), and sodium hydroxide (Ajax Chemicals); hexane (AlliedSignal); and methanol (EM Science). Deuterated methanol (CD_3OD), acetic acid (CD_3COOD), and deuteriotrifluoroacetic acid (*d*-TFA) were obtained from Cambridge Isotope Laboratories. Deuterated water (D_2O) was obtained from ANSTO, Lucas Heights, Sydney, Australia. L-Tyrosine

* Corresponding author (telephone 02 6933 2540; fax 02 6933 2737; e-mail krobards@csu.edu.au).
† Charles Sturt University.
‡ Australian National University.
§ Hebrew University.

10.1021/jf025736p CCC: $22.00
Published on Web 10/04/2002

(ring-3,5-^{3}H) in aqueous ethanol (2%) with an activity of 1887 TBq/mmol (51 Ci/mmol) and unlabeled L-tyrosine (Sigma Chemical Co.) were used in isotopic labeling experiments in conjunction with Ultima Gold MV high flash point liquid scintillation cocktail (Packard, Canberra, Australia).

Phenolic standards were obtained as follows and were used without further purification: apigenin, apigenin 7-glucoside, cyanidin chloride, cyanidin 3-glucoside chloride, luteolin, luteolin 4-glucoside, luteolin 6-glucoside (homoorientin), luteolin 7-glucoside, luteolin 8-glucoside, luteolin 3′,7-diglucoside, and oleuropein from Extrasynthese; caffeic, chlorogenic, *o*-coumaric, *p*-coumaric, ferulic, gallic, homovanillic, sinapic, syringic, and vanillic acids from Sigma Chemical Co.; and tyrosol from Aldrich Chemical Co. In all instances, glycosidic species were *O*-glycosides. All standards were prepared in MeOH/H_2O (50:50 v/v) to the desired concentration and filtered through 0.45 μm plastic, nonsterile filters prior to chromatographic analysis.

Grade 1 water (ISO3696) purified through a Milli-Q water system was used for all chromatographic analyses and sample and standard preparation. Acetone (Ajax Chemicals) and ethanol (CRC Chemicals) were used for cleaning purposes.

Samples. Samples of fruit plus old- and new-season leaves (cv. Hardy's Mammoth) were collected on February 1 and June 15, 1999, from an established grove in Yanco in southwestern New South Wales during the 1999 harvest season. Four trees from the same orchard row were selected on the basis of similarity of tree size, number of branches, and high fruit yields. On each tree, a scaffold, or major branch, was selected for sampling purposes. Each scaffold was facing northeast so as to minimize environmental variability.

Sampling dates corresponded with the time of immature green fruit and mature black fruit, respectively. New-season leaves were defined as those that grow above the fruiting zone and toward the extreme tip of the selected shoot. These leaves had not reached full cuticular development and were still soft. Old season leaves, however, encompassed those leaves that grew between and beyond the fruiting zone toward the tree trunk.

Immature green fruit samples were also taken from trees of the cultivars Corregiola and Verdale, from the same orchard on February 1, 1999. Leaf samples were also collected from the Corregiola cultivar. Green fruit samples were also collected from trees of the cultivar Manzanillo for comparison.

Sample Pretreatment. After sampling, fruit and leaf samples were immediately frozen in liquid nitrogen and were subsequently freeze-dried using a Martin Christ Alpha 1-4 (with controller LDC-1M) freeze-dryer. The freeze-dried olive pulp was removed from the olive stone using a scalpel and diced into small pieces (~8−9 mm^3). The intact olive seed was removed from the stone by crushing. The stone was then macerated into small pieces (~8−9 mm^3) using a hammer. Finally, dried leaves (both old and new season) were cut into small pieces (~4−9 mm^2). All tissues were placed in separate airtight, screw-top plastic jars, and stored at −18 °C prior to analysis.

Extraction Method for Routine Analyses. Dried olive matter (0.25 g of leaf, pulp, seed, or stone) was blended with methanol/water (50:50 v/v; 5 mL) using an Ultra Turrax blender for 20 s. The solution was left to stand for 30 min at ambient temperature and filtered using a Büchner funnel apparatus. The solid mass was recovered and re-extracted as before; however, the solution was left to stand for 15 min prior to filtering. The filtrates were combined and washed with hexane (5 mL). The hexane was discarded and the aqueous phase filtered (GF/F filter paper with a Büchner funnel apparatus, followed by 0.45 μm plastic, nonsterile filters) prior to HPLC analysis.

Hot Extraction. Extraction using heated solvent was used to investigate possible enzyme activity in the fruit extracts. A centrifuge tube containing methanol/water (50:50 v/v; 5 mL) was capped and heated in a hot water bath to 70 °C. Dried green olive pulp (0.25 g; cv. Hardy's Mammoth sampled February 1, 1999) was then added to the tube and immediately blended using an Ultra Turrax blender for 20 s. The tube was recapped and returned to the water bath for 30 min, before being filtered using GF/F filter paper and a Büchner funnel apparatus. The filtrate was recovered, and the solid residue was added to a new centrifuge tube containing solvent at 70 °C and blended for 10 s before being recapped and returned to the water bath for 15 min. This solution was then filtered and combined with the filtrate from the first extraction and left to cool to room temperature before washing with hexane, filtering (GF/F paper followed by 0.45 μm plastic, nonsterile filters), and analyzing by HPLC.

Table 1. Comparison of NMR Spectroscopic Data for Compound **I** and Its Hemiacetal Derivative

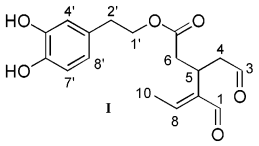

I

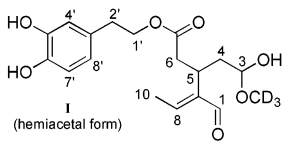

I (hemiacetal form)

proton	this work	Montedoro et al. (*2*)	this work	Montedoro et al. (*2*)
1	9.19	9.19	9.06	9.14
3	9.64	9.62	4.28	4.22
4	2.61, 2.73	2.79	1.71, 1.98	2.00
5	3.63	3.62	3.17	3.24
6a	2.78	2.60	2.68	2.62
6b	2.95	2.90	2.51	2.46
8	6.65	6.61	6.70	6.61
10	2.05	2.04	1.88	1.89
1′	4.19	4.19	4.09, 4.24	4.04
2′	2.77	2.77	2.70	2.65
4′	6.71	6.65	6.67	6.57
7′	6.78	6.70	6.75	6.63
8′	6.60	6.60	6.56	6.45

Spiking. Oleuropein (1.00 mg) was added to dried olive pulp (0.25 g) and extracted as described. The final extract was then analyzed by HPLC. This experiment was conducted to determine whether enzymatic degradation of oleuropein was responsible for the production of **I** (**Table 1**).

Routine High-Performance Liquid Chromatography. HPLC analyses were performed using a Perkin-Elmer binary LC pump 250 equipped with a 20 μL loop injector. A Perkin-Elmer LC-235 diode array detector (280 and 240 nm) and a Perkin-Elmer LC-240 fluorescence detector (excitation, 280 nm; emission, 340 nm) connected in series served to monitor the column eluent. Separation was achieved on a 150 × 4.6 mm i.d., 5 μm Alltima C18 column (Alltech) with gradient elution. The HPLC system was interfaced to a DCM-1488E Lasernet Computer Systems computer and operated using Varian Star (version 4.5) software. The mobile phases were degassed under vacuum using Alltech Nylon 66 membranes and continuously sparged with high-purity helium during analysis to prevent resaturation by air. The gradient elution program employed methanol/acetonitrile/acetic acid (95:5:1 v/v/v) as solvent A and water/acetic acid (100:1 v/v) as solvent B with a flow rate of 1 mL/min. Solvent A was increased linearly from 10% at zero time to 30% at 30 min and then ramped to 40% at 40 min, held isocratically for 5 min followed by further linear ramping to 50% at 50 min with a 5 min isocratic time, and then ramped to 60% at 60 min, to 70% at 65 min, and to 100% at 70 min.

Semipreparative Isolation of Compound I from Hardy's Mammoth Pulp. Olive pulp (2 g, sampled February 1999) was extracted by sonicating with methanol/water/acetic acid (100 mL; 50:50:1 v/v/v) for 30 min. The extract was decanted, and the pulp was re-extracted four times as before. The extracts were pooled, washed with heptane (60 mL), and rotary evaporated using a dry ice/acetone-cooled condenser while the water bath was maintained below 35 °C.

The resulting gum was redissolved in methanol/water/acetic acid (50+50+1 v/v/v; ~5 mL) and sorbed onto an 80 × 20 mm i.d., 35−50 μm Corasil C18 (22 g) column (Waters) that had been pre-equilibrated in the same solvent. The column was eluted with methanol/water/acetic acid (50:50:1 v/v/v; 50 mL), and 10 fractions (5 mL) were collected. These fractions were analyzed by HPLC, and fractions 2−5 (containing the desired peak) were pooled and rotary evaporated to dryness as before. The residue was dissolved in methanol/water/acetic acid (50:50:1 v/v/v; 5 mL) prior to semipreparative separation, which was conducted using a high-pressure mixing gradient system interfaced

with Waters Maxima software. Mobile phase was supplied by two Waters 510 pumps.

Extract (500 μL aliquot equivalent to 200 mg of pulp) was injected manually via a Rheodyne 7125 valve with a 2.4 mL sample loop. Mobile phases A and B consisted of methanol/acetic acid (100:1 v/v) and water/acetic acid (100:1 v/v), respectively. The solvent composition remained at 40% solvent A for 30 min, before a 15 min wash with 100% solvent A, at a constant flow rate of 5 mL/min. A 250 × 10 mm i.d., 5 μm Alltima C18 column (Alltech) was used at 40 °C in a Waters column oven. The column eluate was monitored at 282 nm using a Waters 481 UV detector with a 2.3 mm path flow cell. Fractions were collected manually between 23 and 25 min by observing the detector output on a chart recorder. Fractions were then pooled and rotary evaporated to give 23 mg of an olive green gum (11.5% yield). This was dissolved in methanol/water/acetic acid (50:50:1 v/v/v; 1 mL) and repurified by semipreparative HPLC using isocratic elution at 40% solvent A. Fractions, collected manually, were dried under high vacuum for 1 day and stored at −10 °C under nitrogen, prior to NMR analysis.

Liquid Chromatography—Mass Spectrometry. Sample extracts in methanol/water (50:50 v/v) were analyzed using a Beckman liquid chromatograph (a 126 pump and a 168B diode array detector) and a Micromass Quattro II quadrupole mass spectrometer by electrospray ionization (ESI). A column nominally equivalent to the Alltima C18 column used for HPLC analyses was used in conjunction with the gradient program described for routine HPLC except that solvents A and B contained only 0.1% acetic acid. A flow rate of 1.0 mL/min was used with a split ratio of approximately 20:1 (UV detector/MS). The diode array detector output was monitored at 280 nm by the Masslynx Data System (Micromass) for alignment with the mass spectral data. The mass spectral data were acquired at four alternating scans from *m*/*z* 120 to 800 in 2 s using both positive and negative ion modes at cone voltages of 30 and 70 V.

Nuclear Magnetic Resonance Spectroscopy. Isolated **I** was dissolved in $CD_3OD/D_2O/CD_3COOD$ (50:50:1 v/v/v; 0.8 mL), and the solution was introduced into a 5 mm i.d. tube. One-dimensional ^1H NMR measurements were conducted using a Varian Inova 600 instrument at 600 MHz with a 90° pulse and pulse delay of 5 s. One-dimensional ^{13}C APT NMR measurements were conducted on a Varian Inova 500 instrument at 125 MHz with a pulse delay of 2 s. A further 7 ms pulse was introduced into the total pulse sequence to obtain the 180° phase difference of the methyl and methine carbon signals relative to the methylene and quaternary carbon signals.

Two-dimensional NMR measurements (COSY, HMBC, HMQC, and HMQC-TOCSY) were conducted on the Varian Inova 600 instrument using pulse sequences as supplied by Varian.

Isotopic Labeling Experiments. Olive stems (with no side shoots) ~25 cm long and containing new-season leaves but devoid of fruit were sampled by scalpel from cv. Hardy's Mammoth on April 25, 2001. Additionally, stems with and without black fruits were sampled on June 7, 2001. The stems were placed in separate snap-lock bags and transported on ice from Yanco to Wagga Wagga (150 km), where they were cut at the base at an angle of 45° to an exact length of 25 cm and then weighed (5.0 ± 0.5 g). Leaves were removed from the base of all stems to facilitate stem positioning in scintillation vials, and one stem possessing fruit was stripped entirely of its leaves. Placing the cut end of the stem under running tap water refreshed the shoots. The stems were then placed into glass scintillation vials, containing water (10 mL) and tritium-labeled tyrosine (4625 kBq, ~125 μCi). The scintillation vials were positioned in a 20 cm × 30 cm glass fish tank. A 100 W lamp was shone directly over the fish tank, and a small fan was positioned so as to provide a wind flow across the shoots to enhance their rate of water uptake. Small volumes of water were added to stems as required.

Three of the stems sampled on April 25, 2001, were analyzed after 40 h of uptake, in addition to a control stem. The analysis was repeated using new stems that had experienced uptake for 12 days. Stems possessing leaves and fruits (sampled on June 7, 2001) were sampled only after 12 days of uptake. In leaf extractions, five leaves were sampled from each stem and were cut into 4−16 mm^2 shreds. The shredded leaf (0.5 g) was extracted in the same fashion as previously described for routine analysis. Similarly, for the analysis of fruit samples, pulp (0.5 g) was extracted as described. An aliquot (100 μL) of each extract was used for HPLC analysis using off-line scintillation detection.

High-Performance Liquid Chromatography with Automated Fraction Collection and Off-Line Scintillation Detection. HPLC analyses of extracts from isotopically labeled Hardy's Mammoth stems were performed using a Perkin-Elmer binary LC pump 250 equipped with a 50 μL loop injector, in conjunction with a Perkin-Elmer LC-235 diode array detector (280 nm). Separation was achieved on a 150 × 4.6 mm i.d., 5 μm Alltima C18 column (Alltech) using the same gradient conditions and computer system as outlined for routine HPLC. Fractions (1 mL) were collected using a Gilson FC 203B fraction collector and were subsequently dried in a Gallenkamp vacuum oven (model OVL-570) at 40 °C. Residues were reconstituted with liquid scintillation cocktail (4 mL) prior to being counted using a Tri-Carb liquid scintillation analyzer, model 1600TR (Packard, Canberra, Australia) for 15 min.

RESULTS AND DISCUSSION

Compound Identification. Tissue extracts of cv. Hardy's Mammoth, Corregiola, Verdale, and Manzanillo were analyzed by HPLC with UV and ESI MS detection. Compound identification was based on retention data, fluorescence, UV absorption, and ESI mass spectra where relevant standards were available (**Table 2**). In those instances when authentic standards were unavailable, tentative assignment of structure was based on a systematic search for molecular ions using extracted ion mass chromatograms [computer-generated plots of the abundance of a specific ion extracted from the total ion current (TIC) chromatogram]. ESI LC-MS was performed using two cone voltages, namely, 30 and 70 V, in both positive and negative ion modes, with the higher cone voltage providing additional fragmentation data. Compounds with a presence listed as tentative in **Table 2** were restricted to those instances in which both $[M + H]^+$ and $[M - H]^-$ ions were detected in positive and negative ion ESI, respectively.

Selected ion monitoring at *m*/*z* 541 in positive ion mode showed peaks eluting at 31.0 and 37.1 min with identical positive and negative ion mass spectra. For example, the positive ion spectra exhibited a pseudomolecular ion at *m*/*z* 541 in addition to a sodium adduct peak with fragments at *m*/*z* 137, 165, 207, 225, 243, 361, and 379. This is consistent with the known fragmentation scheme for oleuropein (*8*), which eluted at 31.0 min. The later eluting peak was assigned to the isomeric oleuroside, which was shown by Savournin et al. (*18*) to elute after oleuropein under reverse phase conditions. The mass spectrum of compound **52** (retention time = 21.2 min) exhibited a base peak at *m*/*z* 611 in positive ion mode in addition to a sodium adduct at *m*/*z* 633 and strong peaks at *m*/*z* 449 and 287 due to the loss of one and two glucose moieties, respectively. This mass spectrum was distinct from that of hesperidin, suggesting that stereoisomerism was unlikely. On the other hand, the similarity of the mass spectrum to that of luteolin 3′,7-diglucoside, which eluted, however, at 25.6 min, suggests the possibility of it being an isomer of this diglucoside.

Extracted ion data for *m*/*z* 449 and 447 (positive and negative ions, respectively) showed three peaks with retention times of 28.0, 33.9, and 37.3 min. The peaks at 28.0 and 37.3 min were established from a consideration of the mass spectral and retention data as luteolin 7-glucoside and luteolin 4-glucoside, respectively. The mass spectra exhibited strong pseudomolecular ions (positive and negative ion modes) with strong aglycon peaks corresponding to loss of 162 amu (loss of glucose). The peak eluting at 33.9 min showed almost identical mass spectra (positive and negative ion modes), suggesting that it was a

Table 2. Alphabetical List of Phenolic Compounds with Documented Presence in *O. europaea* Tissues Showing Their Presence or Absence in Hardy's Mammoth Tissues[a]

				tissue										
				pulp		NSL		OSL		seed		stone		
compound	no.	t_r (min)	M	E	L	E	L	E	L	E	L	E	major ESI$^-$ peaks	major ESI$^+$ peaks
I	**34**	27.2	320	R	R	R	R	R	R	R	R	R	165, 195, 319	137, 321
apigenin	**27**	46.1	270											
apigenin 7-glucoside	**24**	32.5	432			T	T		T				179, 199, 269, 431	271, 433, 455
apigenin 7-rutinoside	**28**	31.9	578			T	T	T	T				269, 577	271, 433, 579, 601
caffeic acid	**9**	14.5	180	R		R		R	R	R		R		
5-caffeoylquinic acid	**5**	12.9	354	R	R	R	R	R	R	R	R	R		
cinnamic acid	**29**		148											
o-coumaric acid	**18**	27.3	164											
p-coumaric acid	**11**	20.3	164		R	R	R		R					
cyanidin	**19**	27.5	287											
cyanidin 3-glucoside	**8**	14.3	449											
cyanidin 3-rutinoside	**30**		595											
delphinidin	**31**		302											
delphinidin glucoside	**32**		465											
demethyloleuropein	**33**	21.7	526				T						317, 447, 525	137, 365, 503, 527, 549
elenolic acid	**35**		242											
elenolic acid glucosides	**36**	11.2	404	T	T	T	T	T	T	T	T	T	223, 403	225, 243, 405, 427
		13.4		T	T	T	T	T	T	T	T	T		
		19.6		T	T	T	T	T	T	T	T			
		23.9				T	T	T	T			T		
ferulic acid	**12**	21.5	194											
gallic acid	**1**	4.5	170											
hesperidin	**22**	29.4	610	R	R	R	R	R	R				225, 301, 361, 463, 609	303, 363, 465, 611, 633
homovanillic acid	**6**	13.4	182	R	R	R		R	R	R	R	R		
4-hydroxybenzoic acid	**37**		138											
4-hydroxyphenylacetic acid	**38**		152											
hydroxytyrosol glucoside	**2**	7.0	316	T	T	T	T	T	T	T	T	T	153, 179, 315	155, 317
hydroxytyrosol	**3**	7.3	154	T		T		T		T		T	153, 307	137, 155
ligstroside	**39**	36.5	524	T	T	T	T	T	T	T	T	T	291, 361, 523	363, 525, 547
luteolin	**26**	44.2	286		T	T	T	T	T				141, 179, 285	137, 225, 287
luteolin 4-glucoside	**25**	37.3	448			R	R	R	R				285, 377, 447	137, 287, 449
luteolin 6-glucoside (homoorientin)	**16**	25.2	448											
luteolin 7-glucoside	**21**	28.0	448	R	R	R	R	R	R	R	R	R	285, 447, 377	137, 287, 449
luteolin 8-glucoside	**14**	22.2	448											
luteolin 3′,7-diglucoside	**17**	25.6	610											
luteolin 7-rutinoside	**40**	17.1	594			T	T	T	T				151, 179, 349, 409, 593	153, 225, 457, 595, 617
nüzhenide	**41**	26.9	686		T	T	T	T	T	T	T	T	223, 299, 523, 685	225, 369, 507, 525, 687, 709
oleoside	**42**		331											
oleuropein aglycon	**43**		378											
oleuropein	**23**	31.0	540	R	R	R	R	R	R	R	R	R	223, 275, 307, 377, 539	137, 165, 207, 225, 243, 361, 379, 541, 563
oleuroside	**44**	37.1	540	T	T	T	T	T	T				223, 275, 307, 377, 539	137, 165, 207, 225, 243, 361, 379, 541, 563
protocatechuic acid	**45**		154											
quercitin	**46**		302											
quercetin 3-rhamnoside (quercitrin)	**47**		448											
rutin (quercetin-3-rutinoside)	**48**		610											
salidroside (tyrosol glucoside)	**49**	9.3	300	T	T	T	T		T	T	T	T	227, 299, 599	229, 301, 323, 601
sinapic acid	**13**	21.9	224											
syringic acid	**10**	14.7	198											
tyrosol	**4**	10.3	138	R	R	R	R	R	R	R	R	R		
vanillic acid	**7**	14.0	168	R	R	R	R	R	R	R	R	R		
verbascoside	**15**	24.5	624	T	T	T	T	T	T	T		T	137, 161, 461, 623	163, 325, 625, 647
unknown	**50**	16.2	378	T	T	T	T	T	T	T	T	T	153, 197, 377	199, 217, 379, 401
unknown	**51**	33.9	448	T	T	T	T	T	T	T			285, 377, 447	137, 287, 449
unknown	**52**	21.2	611		T	T	T	T	T				285, 447, 609	287, 449, 611, 633
unknown	**53**	13.0	402	T		T	T	T	T	T			269, 401	177, 195, 229, 357, 403, 425
unknown	**54**	10.5	432	T						T	T	T	213, 257, 431	215, 259, 433, 455
unknown	**55**	14.2	520			T	T	T	T	T			175, 387, 519	177, 209, 339, 389, 521, 543

[a]Identification was based on retention, mass spectral, UV, and fluorescence data as indicated. M, molecular mass; NSL, new season leaves; OSL, old season leaves; E, early season tissues sampled on Feb 1, 1999; L, late season tissues sampled on June 15, 1999. R indicates that presence was confirmed from retention and spectral data of an authentic standard; T indicates tentative identification based on the presence of a pseudomolecular ion in both positive and negative ion ESI. A blank space indicates that there was no evidence for the presence of the compound in that tissue.

luteolin glucoside. This compound was not identified; however, on the basis of retention data it did not arise due to luteolin 6-glucoside (homoorientin) or luteolin 8-glucoside. The possibility that this peak was quercetin 3-rhamnoside (quercitrin) (molecular mass 448) was eliminated from a consideration of mass spectral data as this compound would exhibit an aglycon

peak at *m*/*z* 303 rather than the observed peak at *m*/*z* 287 amu (positive mode). The flavylium forms of cyanidin glucosides, molecular mass 449 amu, will produce $[M]^+$ and $[M - 2H]^-$ ions at 449 and 447, respectively, with ions at *m*/*z* 287 and 285 in positive and negative ion mode, respectively, generated by the corresponding anthocyanidins. Thus, the expected mass spectra for luteolin glucosides and the flavylium form of cyanidin glucosides (and their respective aglycones) will be identical, because these compounds are isobars (*19*). However, retention data established that the unknown peak at 33.9 min was not cyanidin 3-glucoside, and recovery of anthocyanic compounds by the current extraction method is unlikely.

Chromatograms of samples of green Hardy's Mammoth drupes (collected February 1, 1999) were dominated by a large, broad peak, eluting at ~27.2 min using LC-MS conditions. Of significance is the fact that this peak was not attributable to oleuropein, which has been the dominant phenolic compound in green olive fruit (*5*, *13*). However, oleuropein was a minor component in the case of green drupes of cv. Hardy's Mammoth, Corregiola, and Verdale. The high concentration of this unknown compound and the fact that oleuropein was not dominant as expected warranted a full structural characterization by semi-preparative HPLC and multinuclear, multidimensional NMR spectroscopy.

1D ^{1}H NMR spectroscopy conducted on the isolated compound (**Table 1**) was consistent with the structure of the phenol, **I**, identified previously (*2*). Better dispersion of resonances provided by the higher field (600 MHz) compared to that (200 MHz) used by Montedoro et al. (*2*) allowed better resolution of the protons at position 4 (**Table 1**). It is also possible that due to lower resolution, there may have been misassignment of resonances from protons at positions 4 and 6a for **I** (see **Table 1**). The 1D ^{13}C APT spectrum showed 20 signals and was consistent with this structural assignment. An aldehyde carbon was indicated at 198.8 ppm, a carboxyl carbon at 175.1 ppm, and an acetal carbon at 97.9 ppm. Signals between 116 and 146 ppm indicated that olefinic and aromatic systems were probably present. A full structural elucidation involved the use of GC-MS (not reported) and 2D-NMR spectroscopic techniques including through-bond proton-carbon connectivity (HMQC and HMBC) and ^{1}H−^{1}H coupling connectivity (COSY) experiments. HMBC experiments established unequivocally the connectivity between the 3,4-dihydroxyphenylethanol moiety and the deacetoxy elenolic acid moiety as proposed (*2*). NMR spectroscopic experiments (*2*) established internal consistency of these moieties, but connectivity was assumed on the basis of the structure of oleuropein. In nonalcoholic solvents a molecular mass of 320 amu was observed in the mass spectra using direct injection ESI MS. From the composite data, the unknown compound was confirmed as **I** (**Table 1**). A molecular mass of 352 amu was observed when the isolated compound was recovered from alcoholic solvents prior to ESI MS and in the mass spectra from ESI LC-MS using alcoholic mobile phases. NMR experiments in CD_3OD indicated that this compound was a hemiacetal derivative of **I** (**Table 1**).

Compound **I** was first identified in virgin olive oil by Montedoro et al. (*2*). Other authors have identified **I**, but its presence has been restricted to olive products such as oil (*2*, *3*, *15*, *20*), vegetation water and pomace (*1*, *3*), and olive leaves (*21*, *22*). Its presence in the fruit has been specifically excluded by various authors (e.g., ref *2*) and inferred by others (*12*), but the current research is significant as it represents the first definitive report of **I** existing in such high concentrations in pulp and leaf tissues, where it represents the main phenolic

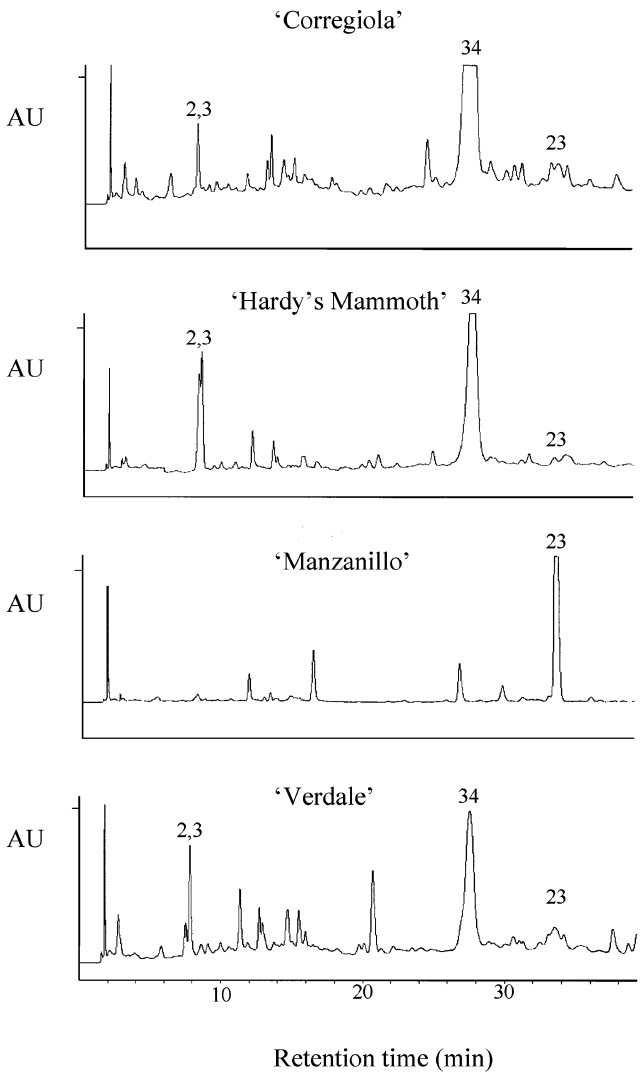

Figure 1. Chromatograms comparing green Corregiola, Hardy's Mammoth, Manzanillo, and Verdale fruits using UV detection at 280 nm. All chromatograms are at a fixed attenuation. Compound numbering corresponds with that in **Table 2**.

present therein. Moreover, previous reports of this compound [variously described as the deacetoxy dialdehydic form of elenolic acid linked to hydroxytyrosol (*2*); oleacein (*21*); and 3,4-dihydroxyphenylethyl 4-formyl-3-formylmethyl-4-hexenoate (*22*)] have attributed its existence to oil-processing methods (*2*, *3*, *15*) and its derivation from oleuropein. Two obvious routes are available for the degradation of oleuropein and related compounds (*11*). First, cleavage by specific esterases gives rise to either elenolic acid glucoside or demethyloleuropein, which are both found in ripe olives. Alternatively, it has been assumed that crushing and malaxation of the olive fruits during oil production activates the endogenous β-glucosidases (*23*), which produce the oleuropein aglycon. Demethyloleuropein derived from esterase activity may also act as a substrate for β-glucosidases (*1*). Various routes have been proposed (*11*, *23*, *24*) for the formation of **I** from the aglycon. For example, it has been proposed that formation from the aglycon occurred via opening of the elenolic ring and successive isomerization of the enolic species to a dialdehydic structure, which was finally decarboxylated (*2*).

Phenolic Profiles of Different Tissues. Profiles of immature green fruits of Hardy's Mammoth, Corregiola, and Verdale (**Figure 1**) were similar and exhibited high concentrations of

hydroxytyrosol and/or hydroxytyrosol glucoside plus **I** (vide infra) but very low concentrations of oleuropein. Conversely, profiles of green Manzanillo fruits were dominated by oleuropein, and neither **I** nor the hydroxytyrosol species were detected as previously reported (*10*) for an earlier fruiting season. Hardy's Mammoth is a uniquely Australian olive cultivar, and from preliminary results using randomly amplified polymorphic DNA it is unrelated to any established cultivars (unpublished data).

The various tissues (new- and old-season leaves, pulp, stone, and seed) of cv. Corregiola (chromatograms not shown) and Hardy's Mammoth were sampled on February 1, 1999 (prior to green maturation), and June 15, 1999, and profiled by HPLC (**Figures 2** and **3**). These chromatograms highlight the differences in the phenolic profiles of the various tissues of cv. Hardy's Mammoth sampled at the same time. The use of TIC chromatograms (or integrated spectral response) provides a more meaningful comparison than that obtained at a single absorption wavelength. Nevertheless, there are some problems with TIC chromatograms as the ionization efficiency varies between phenols, and some phenols, for example, tyrosol (*25*) are not easily ionized. Significant differences are seen in the profiles and also indicated from the literature (e.g., ref *26*). However, most published work has examined a single tissue (*5*−*7*, *27*), and thus comparisons between tissues from different cultivars and times become invalid. Moreover, closer examination of the tissue extracts using extracted ion data showed that the majority of phenols were common to all tissues (**Table 2**) and that the differences evidenced in the profiles are largely the result of quantitative variations between tissues. Nevertheless, leaves contained more glycosylated species and isomeric compounds at detectable concentrations than other tissues.

The dominant phenols in leaf tissues of both Hardy's Mammoth and Corregiola cultivars sampled on February 1 were **I**, luteolin 7-glucoside, oleuropein, and an unidentified phenolic glucoside (compound **51**), with higher concentrations observed in new-season leaves compared to old-season leaves. Profiles of Hardy's Mammoth and Corregiola seeds and stones at the same sampling date were relatively simple, and both tissues contained significantly fewer compounds compared to pulp and leaf tissues. Seed profiles were dominated by salidroside and an unknown phenolic compound (compound **54**) with a molecular mass of 432 amu. Both hydroxytyrosol and its glucoside were also present. In the stone, relatively small concentrations of both hydroxytyrosol species, unknown compound **54**, **I**, and rutin were detected.

There was a significant change in phenolic profiles of all tissues collected at the later sampling date. For example, of the two hydroxytyrosol species only the glucoside was detected in the late-season tissue samples. The profiles of new- and old-season leaves showed much greater similarity in late-season samples. The concentration of **I** declined during fruit maturation and was a minor component in late-season pulp. On the other hand, the concentration of oleuropein increased and was quantitatively the most important phenol in the late-season pulp. The failure to observe **I** previously (*5*, *7*, *13*) may be attributed to extraction conditions (*3*) or cultivar dependence. Given the contradictory findings and our own observations plus the implications from the data of Capasso et al. (*24*) and Hansen et al. (*21*), we pursued the origins of this compound.

Origins of Compound I. The isolation of oleuropein as the major component in drupes of some cultivars but not others suggested the soundness of the isolation procedure. Moreover, oleuropein and not **I** was the major phenolic component of

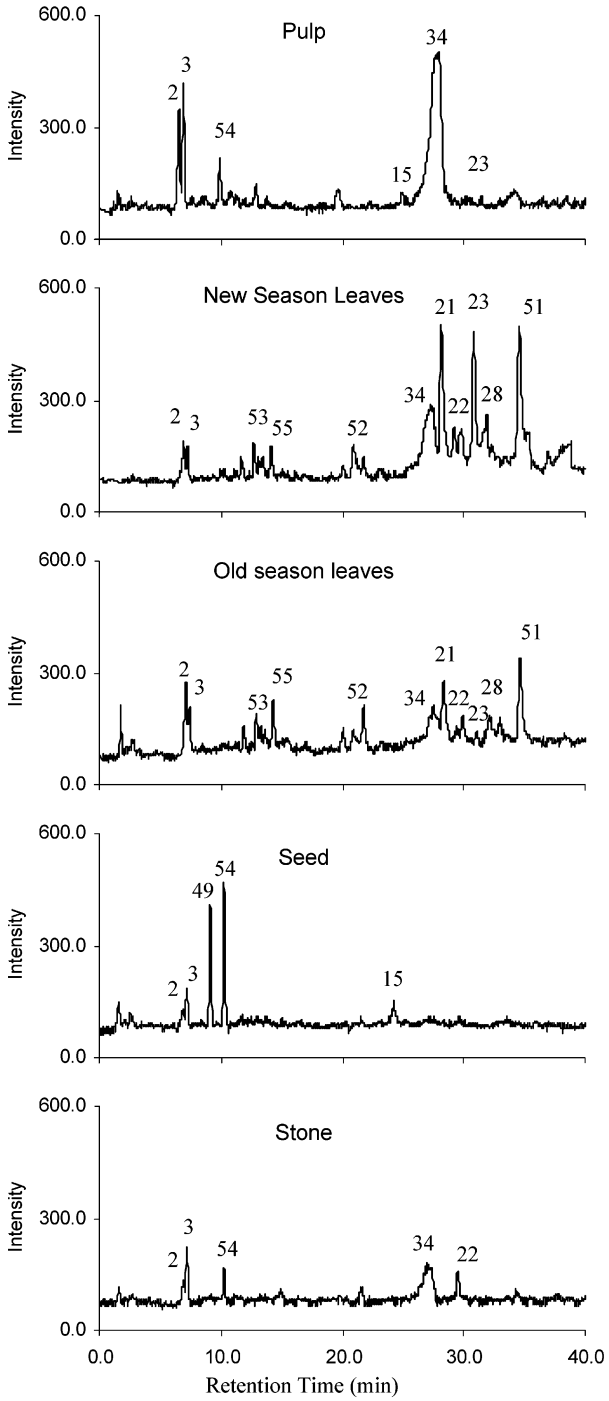

Figure 2. ESI LC-MS chromatograms for Hardy's Mammoth tissues sampled on Feb 1, 1999, in TIC mode (positive ion). Compound numbering corresponds to that presented in **Table 2**.

mature fruit of Hardy's Mammoth. Nevertheless, immature green fruit of cv. Hardy's Mammoth (Corregiola and Verdale) may possess unusually high enzyme activity that favors formation of **I** during extraction. Thus, green olive fruits with a high concentration of **I** were extracted with hot aqueous methanol at 70 °C for 30 min. There was no significant difference in the concentration of **I** obtained in this manner or via the usual extraction procedure. Moreover, the concentration of oleuropein (and other phenols) did not increase following hot extraction. As this process should deactivate any enzymes, it appears to be unlikely that compound **I** arose as an extraction artifact.

Further substantiation that compound **I** did not arise from enzyme activity was obtained by spiking of green drupes of

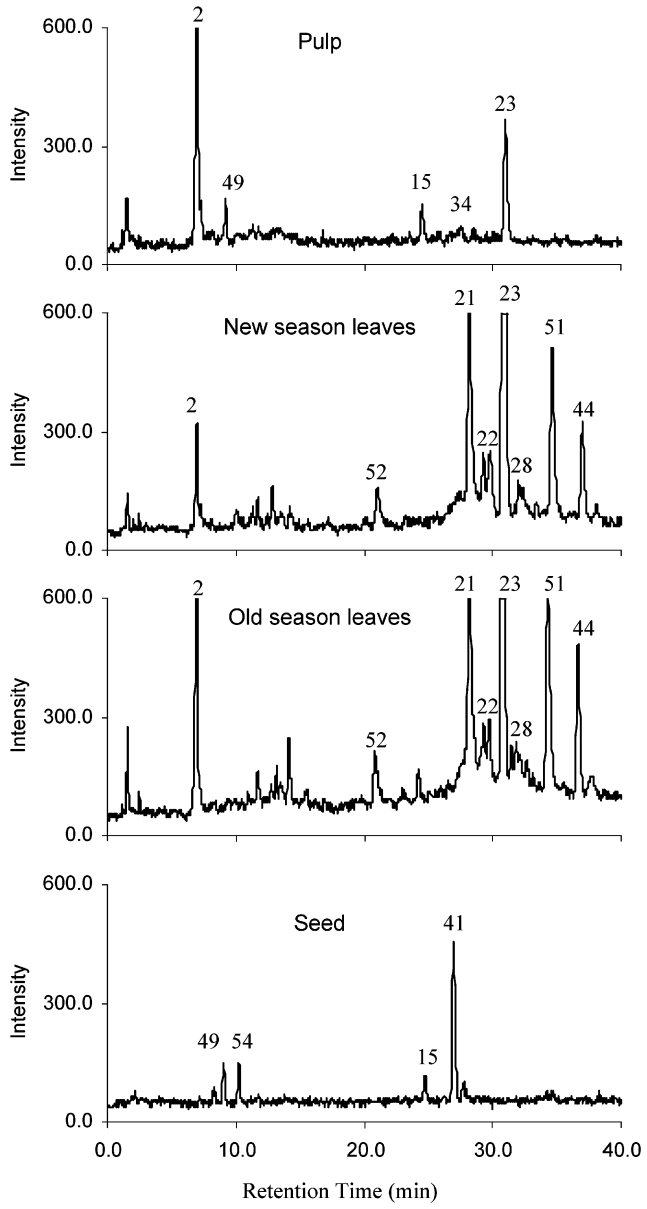

Figure 3. ESI LC-MS chromatograms for Hardy's Mammoth tissues sampled on June 15, 1999, in TIC mode (positive ion). Compound numbering corresponds to that presented in **Table 2**.

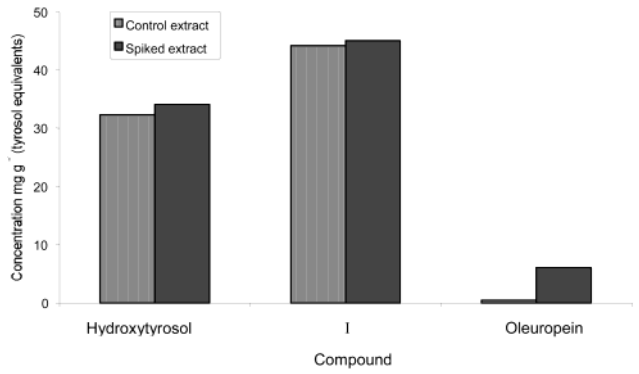

Figure 4. Effect of oleuropein spiking on sample extracts. Data have been expressed as tyrosol equivalents for comparison purposes.

cv. Hardy's Mammoth with oleuropein. Other than the expected increase in oleuropein concentration (**Figure 4**), the chromatograms did not differ from those of unspiked drupes. This finding further supports the conclusion that **I** did not derive from artifactual processes but is present in the drupes.

Isotopic Labeling Investigations. Oleuropein represents a branch point in the mevalonic acid pathway in which terpene synthesis (oleoside moiety) and phenolic synthesis merge. However, the precise origin of oleuropein remains unclear, and isotopic labeling of olive shoots was undertaken to establish a possible relationship between the biosynthesis of **I** and oleuropein (*2*, *3*, *15*, *23*). Thus, tritium-labeled tyrosine from which the phenolic moiety of oleuropein is derived was fed to olive shoots collected on April 25. Problems concerning very slow rates of uptake in *O. europaea* (*17*) were alleviated, but not overcome, by shining a light source directly over the shoots and ensuring that a constant wind source was present. This facilitated shoot transpiration and subsequent uptake.

The uptake of labeled compound was allowed to occur for either 40 h or 12 days in stems with leaves but no fruit. There was no significant incorporation after 40 h, which is attributed to the fact that *O. europaea* is a slow hydroponic absorber of water (*17*) due to its woody tissue. In the stems exposed to 12 days of uptake, significant incorporation occurred in the early-eluting chromatographic fractions and also in peaks eluting at approximately 30 and 41 min. The latter was presumably nonphenolic as it did not absorb in the UV region. The peak eluting at 30 min was identified as **I**, and an activity peak corresponding with the elution of oleuropein was notably absent. Such phenomena are consistent with the high and low concentrations of **I** and oleuropein, respectively, in leaves at this stage of maturation. The data suggest that **I** may be a precursor for the production of oleuropein and that additional time was required if the conversion of **I** to oleuropein was to be observed; however, longer term survival of the tissue became a problem.

In a second experiment, olive stems with both leaves and fruits attached were randomly selected on June 7 to establish the tissue and maturation dependence of the biosynthesis. Prior to labeling experiments, leaves were removed from one set of stems with fruit left intact. Uptake of the isotopically labeled substrate occurred over 12 days, after which time leaves and drupes were analyzed by HPLC using UV and off-line scintillation detection. Fruit tissues were poorly labeled (activity = 3.6 Bq; 100 μL of extract from 5 mL of total extract versus background 1.0 Bq and control labeled substrate = 3.6 Bq) and showed no incorporation of label into phenolic compounds. It appears that biosynthesis of phenolic oleosides and **I** did not occur in olive pulp. On the other hand, significant incorporation of the label occurred in leaves (24.9 Bq), and the incorporation was highest in the shoots containing leaves plus fruit (41.0 Bq), although incorporation was restricted to the leaves. Fractions eluting prior to 10 min once again exhibitied highest activity. This can be attributed to unincorporated tyrosine label and the shunting of the labeled tyrosine into additional biosynthetic pathways. However, a labeled peak eluting at 12 min was identified as tyrosol, implying that tyrosol synthesis can proceed via the pathway proposed in **Figure 5**.

It is interesting to note that activity peaks corresponding to hydroxytyrosol or hydroxytyrosol glucoside were not observed. Our observations are consistent with the findings of Damtoft et al. (*28*), who have suggested that the hydroxytyrosol moiety of oleuropein is formed as a result of ligstroside hydroxylation (scheme 1, **Figure 5**) and that tyrosol represents the major phenolic precursor responsible for the biosynthesis of oleuropein and, presumably, **I**. From our data and others (*17*, *29*), a proposed pathway for the biosynthesis of oleuropein and the structurally similar **I** is presented as scheme 2 of **Figure 5**. The

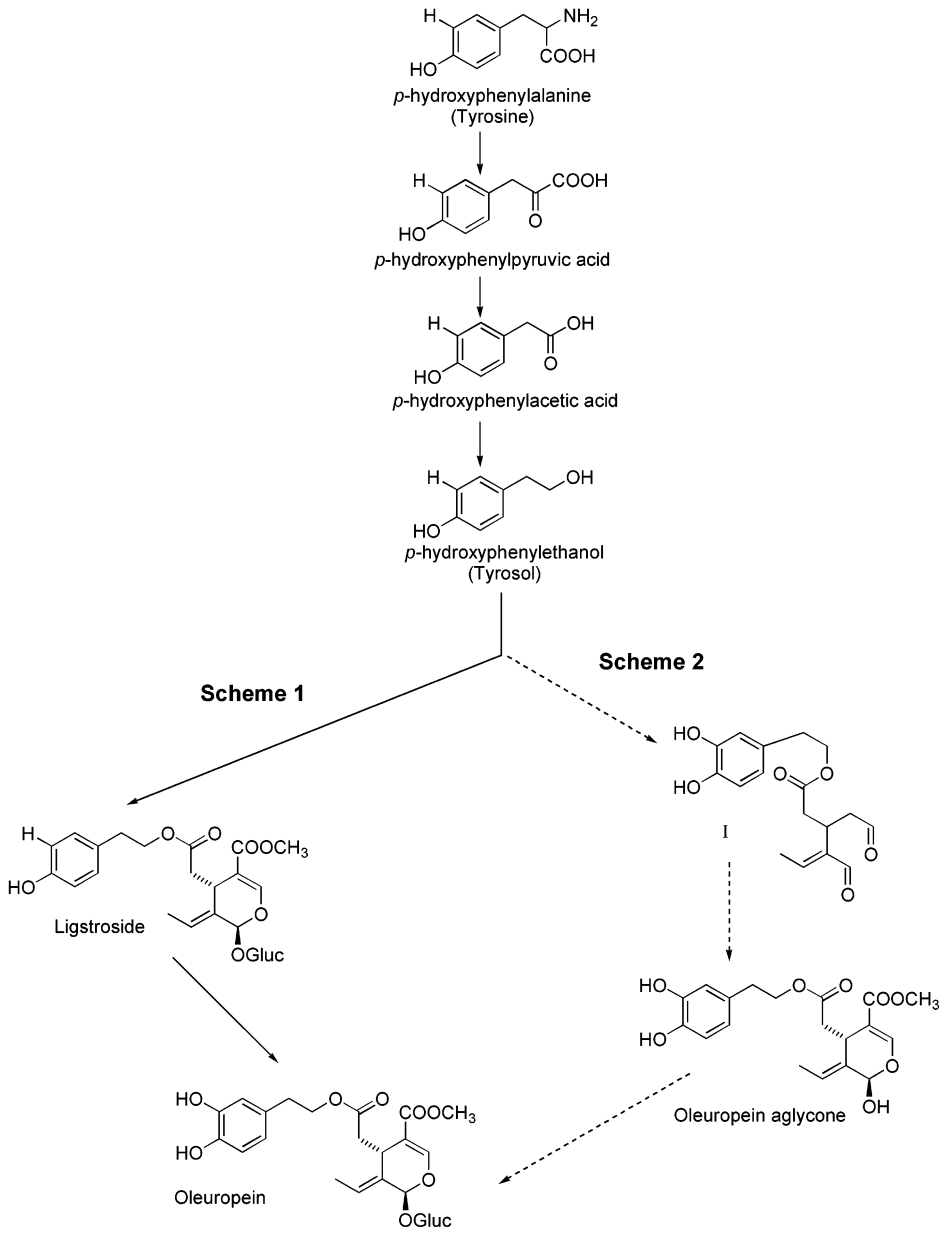

Figure 5. Possible biosynthetic pathway for the production of oleuropein and compound **I**.

data suggest that two biosynthetic routes (schemes 1 and 2, **Figure 5**) are available for the production of oleuropein and that the relative importance of the two is maturation dependent. Our studies of this pathway and the associated enzymes are continuing but are hindered by the difficulty of working with olive tissues as previously observed (*17*). However, the approach adopted in the earlier study of using another species is not a satisfactory solution to our needs.

In summary, the phenolic profiles of tissues of cv. Hardy's Mammoth were found to be qualitatively similar, although profiles of leaf tissues were more complex than those of pulp, seed, or stone. Leaf age did not significantly influence its phenolic profile. Compound **I** was identified as the major phenol in the pulp of green olives of cv. Hardy's Mammoth. The presence of this compound in olive products has previously been attributed to enzymatic degradation of oleuropein by β-glucosidases. However, the current data indicate that its presence is cultivar-dependent and probably functions as a precursor of oleuropein. Further studies of genetically related cultivars are clearly warranted. Moreover, the effect of season and environment on the bioformation of this compound should be investigated.

ACKNOWLEDGMENT

The assistance of Trevor McLean in the fractionation of **I** is gratefully acknowledged.

LITERATURE CITED

(1) Lo Scalzo, R.; Scarpati, M. L. A new secoiridoid from olive wastewaters. *J. Nat. Prod.* **1993**, *56*, 621−623.

(2) Montedoro, G.; Servili, M.; Baldioli, M.; Selvaggini, R.; Miniati, E.; Maccioni, A. Simple and hydrolyzable compounds in virgin olive oil. 3. Spectroscopic characterizations of the secoiridoid derivatives. *J. Agric. Food Chem.* **1993**, *41*, 2228−2234.

(3) Servili, M.; Baldioli, M.; Selvaggini, R.; Miniati, E.; Macchioni, A.; Montedoro, G. High-performance liquid chromatography evaluation of phenols in olive fruit, virgin olive oil, vegetation waters, and pomace and 1-D and 2-D-nuclear magnetic resonance characterization. *J. Am. Oil Chem. Soc.* **1999**, *76*, 873−882.

(4) Visioli, F.; Bellosta, S.; Galli, C. Oleropein, the bitter principle of olives, enhances nitric oxide production by mouse macrophages. *Life Sci.* **1998**, *62*, 541−546.
(5) Amiot, M.-J.; Fleuriet, A.; Macheix, J.-J. Importance and evolution of phenolic compounds in olive during growth and maturation. *J. Agric. Food Chem.* **1986**, *34*, 823−826.
(6) Amiot, M.-J.; Fleuriet, A.; Macheix, J.-J. Accumulation of oleuropein derivatives during maturation. *Phytochemistry* **1989**, *28*, 67−69.
(7) Esti, M.; Cinquanta, L.; La Notte, E. Phenolic compounds in different olive varieties. *J. Agric. Food Chem.* **1998**, *46*, 32−35.
(8) Ryan, D.; Robards, K.; Prenzler, P.; Jardine, D.; Herlt, T.; Antolovich, M. Liquid chromatography with electrospray ionisation mass spectrometric detection of phenolic compounds from *Olea europaea*. *J. Chromatogr. A* **1999**, *855*, 529−537.
(9) Ryan, D.; Robards, K.; Lavee, S. Determination of phenolic compounds in olives by reversed-phase chromatography and mass spectrometry. *J Chromatogr. A* **1999**, *832*, 87−96.
(10) Ryan, D.; Robards, K.; Lavee, S. Changes in phenolic content of olive during maturation. *Int. J. Food Sci. Technol.* **1999**, *34*, 265−274.
(11) Ryan, D.; Antolovich M.; Prenzler, P.; Robards, K.; Lavee, S. Biotransformations of phenolic compounds in *Olea europaea*. *Sci. Hortic.* **2002**, *92*, 147−176.
(12) Bianco, A. D.; Muzzalupo, I.; Piperno, A.; Romeo, G.; Uccella, N. Bioactive derivatives of oleuropein from olive fruits. *J. Agric Food Chem.* **1999**, *47*, 3531−3534.
(13) Brenes, M.; Garcia, P.; Duran, M. C.; Garrido, A. Concentration of phenolic compounds change in storage brines of ripe olives. *J. Food Sci.* **1993**, *58*, 347−350.
(14) Duran, R. M.; Cabello, R. L.; Gutierrez, V. R.; Fiestas, P.; Vàzquez Roncero, A. Bitter phenolic glucosides from seeds of olive (*Olea europaea*). *Grasas Aceites* **1994**, *45*, 332−335.
(15) Servili, M.; Baldioli, M.; Selvaggini, R.; Macchioni, A.; Montedoro, G. Phenolic compounds of olive fruit: One- and two-dimensional nuclear magnetic resonance characterization of nüzhenide and its distribution in the constitutive parts of fruit. *J. Agric. Food Chem.* **1999**, *47*, 12−18.
(16) Akillioglu, M.; Tanrisever, A. Description of phenolics in olive trees and determination of composition in two different organs and cultivars. *Olivae* **1997**, *68*, 28−31.
(17) Damtoft, S.; Franzyk, H.; Jensen, S. R. Biosynthesis of secoiridoid glucosides in *Oleaceae*. *Phytochemistry* **1993**, *34*, 1291−1299.
(18) Savournin, C.; Baghdikian, B.; Elias, R.; Dargouth-Kesraoui, F.; Boukef, K.; Balansard, G. Rapid high-performance liquid chromatography analysis for the quantitative determination of oleuropein in *Olea europaea* leaves. *J. Agric. Food Chem.* **2001**, *49*, 618−621.
(19) Favretto, D.; Flamini, R. Application of electrospray ionization mass spectrometry to the study of grape anthocyanins. *Am. J. Enol. Vitic.* **2000**, *51*, 55−64.
(20) De Nino, A.; Mazzotti, F.; Perri, E.; Procopio, A.; Raffaelli, A.; Sindona, G. Virtual freezing of the hemiacetal-aldehyde equilibrium of the aglycones of oleuropein and ligstroside present in olive oils from *Carolea* and *Cortina* cultivars by ionspray ionization tandem mass spectrometry. *J. Mass Spectrom.* **2000**, *35*, 461−467.
(21) Hansen, K.; Andersen, A.; Christensen, S. B.; Jensen, S. R.; Nyman, U.; Smitt, U. W. Isolation of an angiotensin converting enzyme (ACE) inhibitor from *Olea europaea* and *Olea lancea*. *Phytomedicine* **1996**, *2*, 319−325.
(22) Paiva-Martins, F.; Gordon, M. H. Isolation and characterization of 3,4-dihydroxyphenylethyl-4-formyl-3-formylmethyl-4-hexenoate from olive (*Olea europaea*) leaves. *J. Agric. Food Chem.* **2001**, *49*, 4214−4219.
(23) Vierhuis, E.; Servili, M.; Baldioli, M.; Schols, H. A.; Voragen, A. G. J.; Montedoro, G. Effect of enzyme treatment during mechanical extraction of olive oil on phenolic compounds and polysaccharides. *J. Agric. Food Chem.* **2001**, *49*, 1218−1223.
(24) Capasso, R.; Evidente, A.; Visca, C.; Gianfreda, L.; Maremonti, M.; Greco, G., Jr. Production of glucose and bioactive aglycone by chemical and enzymatic hydrolysis of purified oleuropein from *Olea europea*. *Appl. Biochem. Biotechnol.* **1996**, *61*, 365−377.
(25) McDonald, S.; Prenzler, P. D.; Antolovich, M.; Robards, K. Phenolic content and antioxidant activity of olive extracts. *Food Chem.* **2000**, *73*, 73−84.
(26) Limiroli, R.; Consonni, R.; Ranalli, A.; Bianchi, G.; Zetta, L. ^{1}H NMR study of phenolics in the vegetation waters of three cultivars of *Olea europaea*: Similarities and differences. *J. Agric. Food Chem.* **1996**, *44*, 2040−2048.
(27) Vlahov, G. Flavonoids in three olive (*Olea europaea*) fruit varieties during maturation. *J. Sci. Food Agric.* **1992**, *58*, 157−159.
(28) Damtoft, S.; Franzyk, H.; Jensen, S. R. Biosynthesis of iridoids in *Syringa* and *Fraxinus*: Secoiridoid precursors. *Phytochemistry* **1995**, *40*, 773−784.
(29) Mann, J. In *Secondary Metabolism*, 2nd ed.; Clarendon: Oxford, U.K., 1978.

Received for review June 13, 2002. Revised manuscript received September 6, 2002. Accepted September 6, 2002. Financial assistance by Rural Industries and Horticultural Research and Development Corporations and Australian Research Council is acknowledged.

JF025736P